Available online www.jsaer.com

Journal of Scientific and Engineering Research, 2020, 7(11):141-149

Review Article

ISSN: 2394-2630
CODEN(USA): JSERBR

Correlative study between geotechnical characteristics and indices of water erosion of cultivated or non-cultivated land of the plateau of Thiès. (Senegal)

Abdoulaye Diédhiou[1,2], Mamadou L. Lo[1], Papa B. D. THIOUNE[1,3], El Hadji B. DIAW[1*]

[1]Laboratory of Science and Technology of Water and Environment (LaSTEE), Polytechnic School of Thies BP A10 Thiès, Senegal, (elhbdiaw@ept.sn*);
[2]Ecole Supérieure Polytechnique, UniversitéCheikh Anta Diop de Dakar, corniche Ouest BP 5085 Dakar-Fann
[3]University Alioune DIOP of Bambey, Higher Institute of Agricultural and Rural Training (ISFAR) PO Box 54, Bambey, Senegal

Abstract Water erosion is a natural phenomenon on that can worsen under the combined action weather conditions; this form of diffuse pollution is often measured by the qualities of sediments exported to the watersheds outlet. In general, water erosion will depend on the importance of the frequency of the agents of erosion (rain and runoff), the soil types, topography and the occupation of the territory. The objective of this work is to make a correlative study between the geotechnical characteristics and indices of water erosion of cultivated (or not) land of the plateau of Thiès. The results showed us that according to the system of soils classification of the Central of bridges and Roadways laboratory, samples taken in the polls are composed of: 45% of clayey grave; 25% of silty sand; 21% of clayey sand; 9% of highly plastic clay. On the one hand, there is a good correlation between the index of structural stability of Henin and the limits of consistency on the 0-20 cm horizon (that is the index of structural stability of Henin and the liquid limit, the index of structural stability of Henin and the plasticity limit, finally the index of structural stability of Henin and the plasticity index); On the other hand, we note a poor correlation between the index of structural stability of Henin and the limits of consistency on the 20-40 cm horizon.

Keywords Kissane, water, soil, erosion, correlation

Introduction

For more than a decade there has been a downward trend in the rate of growth of world agricultural production, particularly in cereals. Indeed, after an average increase of 2.3% per year between 1950 and 1984, cereal yields increased by only 1.8% per year between 1980-84 and by 0.5% in the 1990s, less than one-third of the world's population growth rate. This decrease is mainly attributed to accelerated soil degradation [1]. This degradation of soils ranges from pollution to salinization caused by the misuse of chemicals (fertilisers, pesticides, etc.) through erosion resulting from bad farming practices. Erosion is the most common form of soil degradation. According to empirical estimates made on an annual basis, it results in an average of 5 to 10 tonnes of soil per hectare in Africa, Europe and Australia, from 10 to 20 tonnes per hectare across the American continent, and nearly 30 tonnes per hectare in Asia [1]. This process of accelerated soil degradation in several regions of the world is also very present in Senegal [2-3]. The main objective of this work is to conduct a correlative study between geotechnical characteristics and signs of water erosion of cultivated and uncultivated soils of the Thiès plateau: through an application to the Kissane watershed [2, 4]. The methodology is based on theoretical developments based on numerous experimental works identified in the literature [5].

Materials and Methods

Description of the study area

The rural commune of NottoDjobass is located in the center of the region of Thiès it is located 12 km from the city of Thiès and limited to the North-West by the rural commune of Fandène, in the North-East by Thiéneba, to the south by the rural commune of Tassette and the department of Mbour and finally to the west by the rural commune of Keur Moussa. The rural commune comprises 67 villages and covers an area of 252.1 km^2. Its population is estimated at 49,614 [2]. The study area relates more specifically to the village of Kissane. The rural commune is subdivided into five (05) Zones: Zone 1: Baback, Zone 2: Pout Diack, Zone 3: Hanène, Zone 4: Sanghé, Zone 5: Nottodiobass.

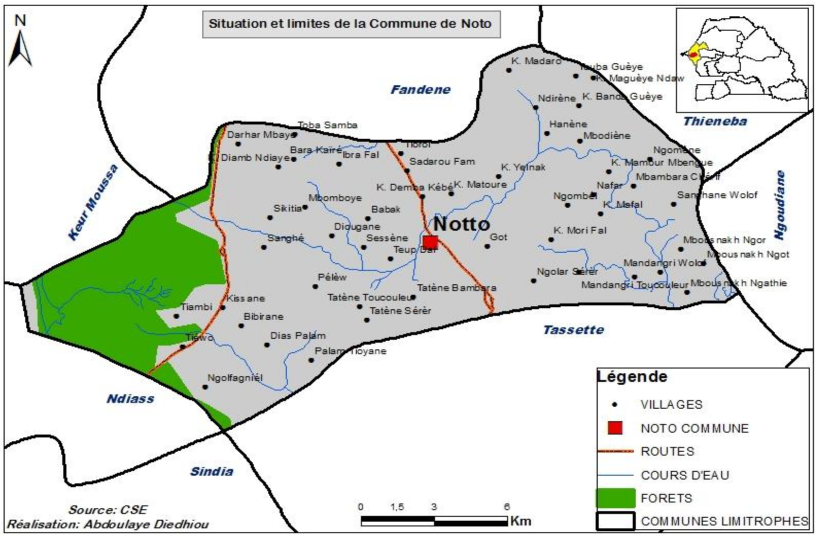

Figure 1: Location of the study area

Methodology

Field campaigns will be conducted to collect soil samples from the Kissane watershed. From topographical maps and information from the literature, we will target survey sites that will be the subject of these field campaigns. The samples collected were tested at the Laboratory of Science and Technology of Water and Environment (LASTEE) – EPT in accordance with the geotechnical program including the following tests:

- Granulometry by sieving;
- The limits of consistency or Atterberg;
- The equivalent sand test if the limits are indeterminable;
- Determination of organic matter content;
- Henin Structural Stability Index.

Using the Principal Component Analysis (CPA) statistical method, variable/individual data can be described when individuals are described by a large number of variables [6]. In such a situation, there is no graphical representation to visualize a point cloud formed by these data. The technique of the principal component analysis then makes it possible to detect the most relevant affinities between the variables and to reduce those which represent only noise. The data are represented in the form of a table or the rows indicate the values taken by the individuals and the columns constitute the variables that are the properties of the different materials. When the coordinates of the individual's cloud points are large, the origin should be chosen wisely. The point O corresponding to the origin shall be linked to the centre of gravity of the point cloud. Therefore, the centre of gravity is defined as the point such that:

$$\sum_{i=1}^{n} pi\overline{Gui} = \vec{0} \quad (1)$$

Based on geometrical aspects, the ACP is particularly interested in distances between individuals in order to interpret condensation and dispersions contained in a cloud of points. This is equivalent to measuring the distance between each pair of individuals. The concept of distance in statistics corresponds to an individual whose components do not bear homogeneous units. In this case, the formula of Pythagoras is no longer valid to determine it. In ACP, classical Euclidean distance is used to represent units in space [7]. The distance between two units ui and ui' can be expressed by the following relation:

$$d^2(u_i, u_i^{/}) = \sum_{j=1}^{p}(xij - xi'j)^2 \quad (2)$$

Each variable xj is a list of n values, so it is considered as an xj vector of an E space with n dimensions called the space of variables. In the space of the variables one is interested in the angles between the vectors because of considering that the coefficient of linear correlation is simply the cosine of the angle between two centered variables. Thus, between two vectors $\overrightarrow{OU}_1 et \overrightarrow{OU}_{1'}$ is associated the scalar product:

$$(\overrightarrow{OU}_1; \overrightarrow{OU}_{1'}) = \sum_{j=1}^{p} X_{ij} X_{i'j} = U_i^T U_{i'} \quad (3)$$

The norm of the vector $\overrightarrow{OU}_1$ is:

$$\overrightarrow{OU}_1 = \sum_{j=1}^{p}(x_{ij} - x_{i'j})^2 \quad (4)$$

The angle between two vectors is given by its cosine by the expression:

$$\cos(\alpha) = \frac{(\overrightarrow{OU}_1; \overrightarrow{OU}_{1'})}{\left\|\overrightarrow{OU}_1\right\| \left\|\overrightarrow{OU}_{1'}\right\|} = \frac{\sum_{j=1}^{p} xij\ xi'j}{\sqrt{\sum_{j=1}^{p} x^2 ij \sum_{j=1}^{p} x^2 xi'j}} = \frac{U_i^T U_i}{\sqrt{U_i^T U_i U_{i'}^T U_{i'}}} \quad (5)$$

The moment of inertia is used to disperse the cloud of individuals from the centre of gravity. The greater the moment of inertia, the more scattered the cloud of points. Contrary to this, the cloud of points concentrated around the centre of gravity results in a weak moment of inertia. At a point b, inertia can be calculated by the relation given by Huygens:

$$I_b = I_G = \left\|G - b\right\|^2 \quad (6)$$

I_G Can be written in the form:

In this form, it can be seen that total inertia is equal to the trace of the covariance matrix

$\sum$ of p variables

$$I_G = trace(\sum) \quad (7)$$

The representation of variables and individuals is made of a similar matter it suffices to make the reasoning in Rn instead of Rp. Variables do not have the same meaning as individuals; after representing individuals in the space of the old variables, a basic change is made in this space [8]. The new axes are linear combinations of the old axes and can therefore be considered as new linear combinations of the old ones. These new variables rated C1, C2, ..., Ck,..., Cp are the main components. Either: Ck the new variable corresponding to the Ak axis:

$$C_k = \sum_{j=1}^{p} \alpha_{kj} V_{Ctj} = X_{ctj} = X_{ct} \alpha_k \quad (8)$$

It is interesting to see how the old variables are related to the new ones and for this we calculate the correlations of the old variables with the new ones.

The correlation coefficient between the old and new variables represents the coordinates of the old variables. So the representation is done on a circle called "circle of correlations", which comes from the fact that a correlation coefficient varying between -1 and 1, the representations of the starting variables are points within a circle of radius 1.

- The ACP is performed between the particle size fractions (%Passing 2 mm, 0.2 mm and 0.08 mm) and the Hénin;
- The Limits of Consistency and the indices of Hénin;
- As well as the Hénin Stability Index.

The interpretation of correlation circles is to identify the angle formed between two variables. This angle is measured by the cosine and is equal to the linear correlation coefficient between two variables. An angle less than 90° shows that these variables are positively correlated. If they are opposite, they are negatively correlated. A lack of correlation results in a right angle formed by the two variables.

Results and Discussions

Determination of Atterberg limits

The consistency limits are water content that cause changes in states [9].

Table 1: Atterberg Limits (0-20)

Sample N°	S15-1	S20-2	S28-1	S31-1	S43-1	S45-1
Horizon (cm)	0-20	0-20	0-20	0-20	0-20	0-20
Liquid limit	23.2	43.3	44.4	129	37.4	33.3
Plastic limit	14.7	24.1	27	60.1	24	23.1
Plasticity index	8.6	19.2	17.4	68.9	13.4	10.3

Table 2: Atterberg Limits horizon (20-40)

Sample N°	S7-1	S7-2	S8-2	S9-2	S10-2	S16-1
Horizon (cm)	20-40	20-40	20-40	20-40	20-40	20-40
Liquid limit	20.5	36.1	22.4	35.3	30.3	21.6
Plastic limit	15.8	20	15.6	19.2	18.6	14.6
Plasticity index	4.6	16.1	6.8	16.2	11.7	6.9

Table 3: Atterberg Limits horizon (20-40)

Sample N°	S16-2	S18-1	S18-2	S19-1	S19-2	S19-2
Horizon (cm)	20-40	20-40	20-40	20-40	20-40	20-40
Liquid limit	20.1	26.3	22.3	51.3	72.2	72.2
Plastic limit	15.5	14.8	14.6	28.9	37.4	37.4
Plasticity index	4.6	11.5	7.6	22.4	34.7	34.7

Table 4: Atterberg Limits horizon (20-40)

Sample N°	S21-1	S21-2	S23-1	S24-1	S25-1	S26-1
Horizon (cm)	20-40	20-40	20-40	20-40	20-40	20-40
Liquid limit	36.1	51	46.8	57.3	31.3	45.5
Plastic limit	22.2	28.2	25.8	35.2	18.6	29.4
Plasticity index	14	22.8	21	22.2	12.7	16.1

Table 5: Atterberg Limits horizon (20-40)

Sample N°	S27-1	S27-2	S29-1	S30-1	S32-1	S33-1
Horizon (cm)	20-40	20-40	20-40	20-40	20-40	20-40
Liquid limit	62.8	67.3	31.5	41.7	47.2	66.5
Plastic limit	32.3	34.2	18.4	29.2	32	43
Plasticity index	30.5	33.1	13.1	12.5	15.2	23.4

Table 6: Atterberg Limits horizon (20-40)

Sample N°	S33-2	S34-1	S35-1	S36-1	S43-2	S45-2
Horizon (cm)	20-40	20-40	20-40	20-40	20-40	20-40
Liquid limit	87.2	38.4	49.3	36.5	183.4	98
Plastic limit	46.5	24.1	29.2	25	60.6	38.6
Plasticity index	40.7	14.3	20.1	11.5	122.9	58.4

Hénin structural stability test

The structural stability of soils is an essential component of their resistance to erosion, which is why structural stability tests are among the most reliable indicators of soil erosion. The Henin test has the advantage of simultaneously integrating the action of several deconstructing agents (bursting and swelling-dispersion) [10].

This test comprises on the one hand particle size type analyses and on the other hand a measurement of the filtration speed, all of which must be carried out under standardised conditions and according to a precise protocol [11]. Particle size analyses are intended to determine the weight fractions of aggregates with a diameter greater than 0.2 mm remaining after immersion in water of an untreated sample Ag_E and of alcohol Ag_A and benzene Ag_B pre-treated samples respectively, and the particle size fractions with a diameter of less than 0.02 mm and between 0.2 and 2 mm (coarse sand, S_g) [11-12]. These various parameters allow the determination of a structural instability index I_s defined by:

$$I_S = \frac{Fraction\ \phi < 0{,}02\,mm}{\frac{Ag_A + Ag_B + Ag_E}{3} - 0{,}9\,S_g} \quad (9)$$

Together with the measurement of the filtration rate, this index provides a good indication of the structural stability of a soil. The higher the value of the Henna structural instability index (it varies globally between 0.1 and 100) and the more the soil tends to disintegrate to clog itself under the effect of water circulation, which reduces the rate of filtration, so that these two parameters vary in the opposite direction.

Table 7: Hénin Structural Stability Test (Horizon 0-20 cm)

Sample N°	Horizon (cm)	Hénin Structural Stability
S 2-1	0- 20	0.13
S 7-1	0- 20	0.07
S 8-1	0 – 20	0.27
S 11-1	0 – 20	0.12
S 15-1	0 – 20	0.34
S 16-1	0 – 20	0.30
S 18-1	0 – 20	0.39
S 20-2	0 – 20	0.88
S 21-1	0 – 20	0.93
S 22-1	0 – 20	0.36
S 27-1	0 – 20	1.05
S 28-1	0 – 20	0.40
S 31-1	0 – 20	1.56
S 33-1	0 – 20	1.17
S 43-1	0 – 20	0.60
S 45-1	0 – 20	0.77

Table 8: Hénin Structural Stability Test (Horizon 20-40 cm)

Sample N°	Horizon (cm)	Hénin Structural Stability
S 7-2	20 – 40	0.35
S 8-2	20 – 40	1.85
S 9-2	20 – 40	1.13
S 10-2	20 – 40	0.13
S 16-1	20 – 40	0.30
S 16-2	20 – 40	0.38
S 18-1	20 – 40	0.39
S 18-2	20 – 40	0.52

S 19-1	20 – 40	0.60
S 19-2	20 – 40	1.47
S 21-1	20 – 40	0.93
S 21-2	20 – 40	0.56
S 23-1	20 – 40	0.71
S 25-1	20 – 40	0.38
S 26-1	20 – 40	0.27
S 27-1	20 – 40	1.05
S 27-2	20 – 40	0.99
S 29-1	20 – 40	0.27
S 30-1	20 – 40	0.33
S 32-1	20 – 40	0.74
S 33-2	20 – 40	1.67
S 34-1	20 – 40	0.80
S 36-1	20 – 40	0.87
S 43-2	20 – 40	1.18
S 45-2	20 – 40	2.22

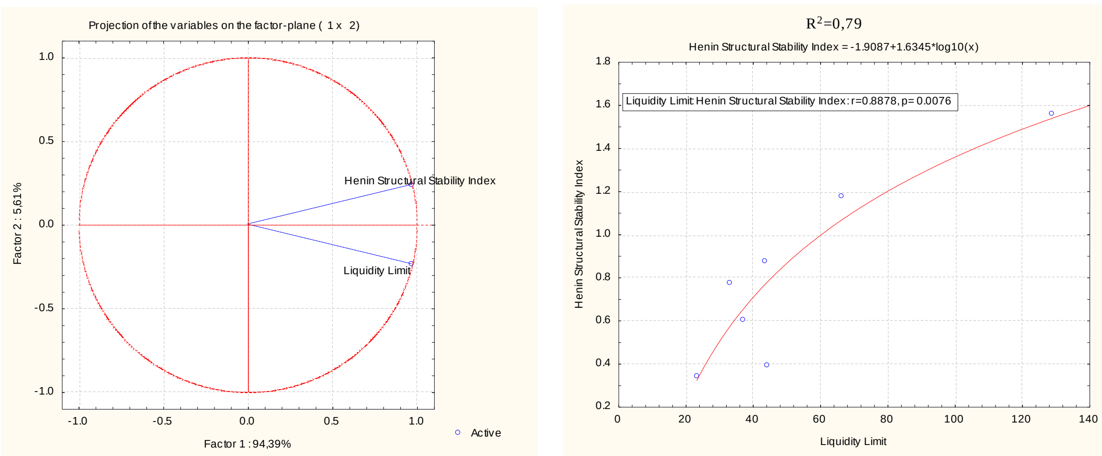

Figure 2: Relationship between the Hénin Structural Stability Index and the Liquidity Limit (horizon 0-20 cm)

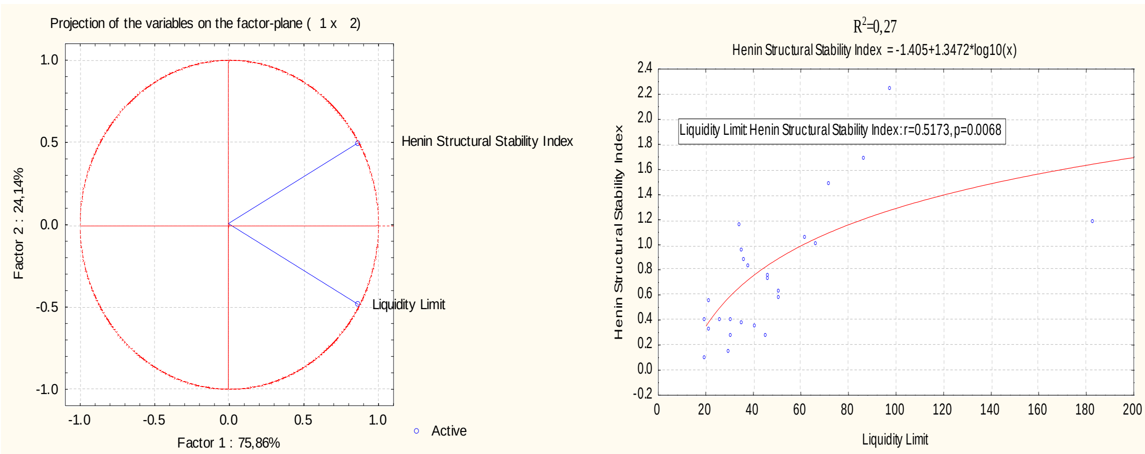

Figure 3: Relationship between the Hénin Structural Stability Index and the Liquidity Limit (horizon 20-40 cm)

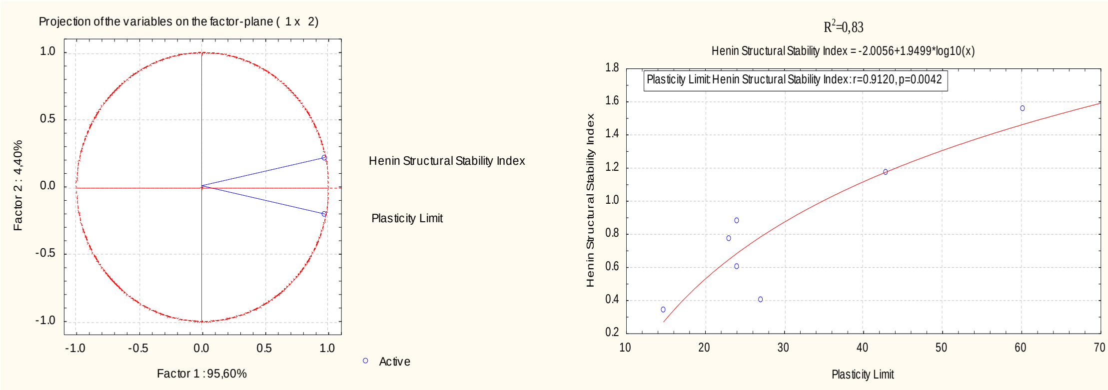

Figure 4: Relationship between the Henin Structural Stability Index and the Plasticity Limit (horizon 0-20 cm)

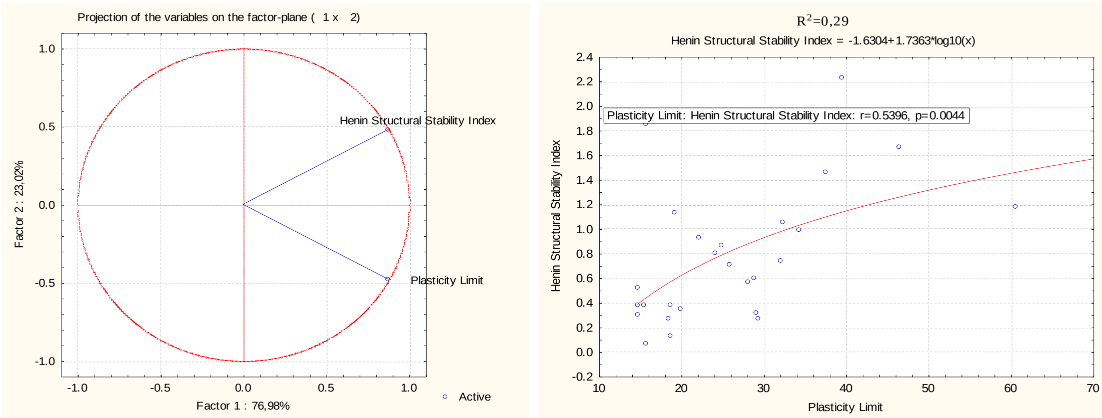

Figure 5: Relationship between the Hénin Structural Stability Index and the Plasticity Limit (horizon 20-40 cm)

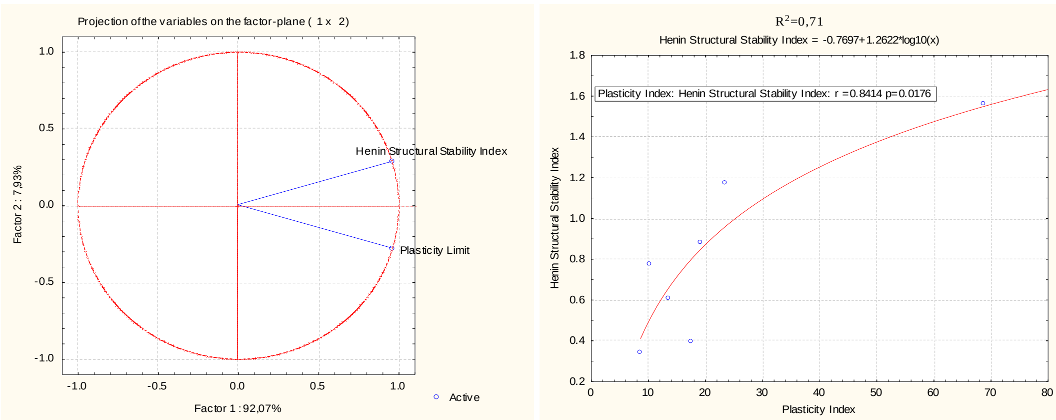

Figure 6: Relationship between the Hénin Structural Stability Index and the Plasticity Limit (horizon 0-20 cm)

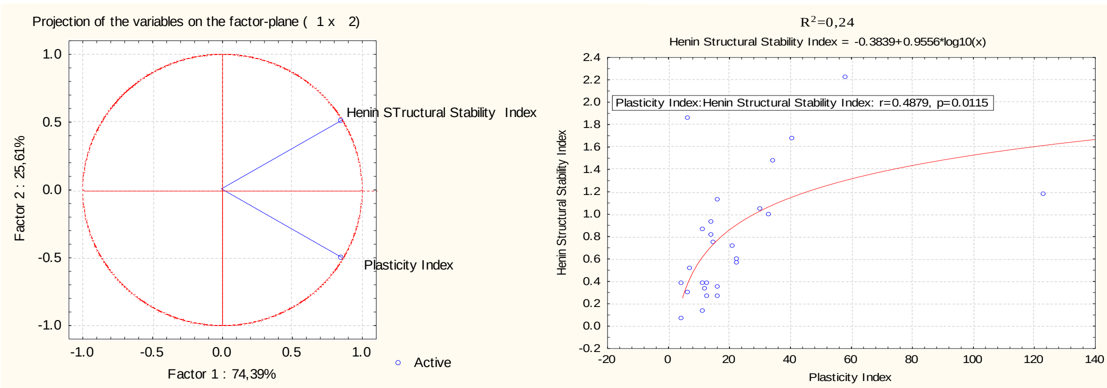

Figure 7: Relationship between the Henin Structural Stability Index and the Plasticity Index (horizon 20-40 cm)

Discussions

- Axis 1 summarizes 94.39% of the information obtained with the two variables. Interpretation of the correlation circle between the Henin's structural stability index and the liquidity limit of the horizon 0-20 cm (fig.2) consists in identifying the angle formed between these two variables. This angle θ is equal to 28.35° less than 90° ($r_{Z_1 Z_2} = 0.88$), which means that these two variables are positively correlated.
- Figure 3 shows that axis 1 summarizes 75.86% of the information obtained with the two variables. Interpretation of the correlation circle between Henin's structural stability index and the liquidity limit of the horizon 20-40 cm gives an angle θ tending to 58.66° less than 90° ($r_{Z_1 Z_2} = 0.52$), which means that these two variables are positively correlated.
- Figure 4 shows that axis 1 summarizes 95.60% of the information obtained with the two variables. Interpretation of the correlation circle between Henin's structural stability index and the plasticity limit of the horizon 0-20 cm gives an angle θ equal to 24.49° below 90° ($r_{Z_1 Z_2} = 0.91$), which means that these two variables are positively correlated.
- Figure 5 shows that axis 1 summarizes 76.98% of the information obtained with the two variables. Interpretation of the correlation circle between Henin's structural stability index and the plasticity limit of the 20-40 cm horizon gives an angle equal to 57.32° less than 90° ($r_{Z_1 Z_2} = 0.54$), which means that these two variables are positively correlated.
- Figure 6 shows that axis 1 summarizes 92.07% of the information obtained with the two variables. Interpretation of the correlation circle between Henin's structural stability index and plasticity index of the 0-20 cm horizon gives an angle equal to 32.86° less than 90° ($r_{Z_1 Z_2} = 0.84$), which means that these two variables are positively correlated.
- Figure 7 shows that axis 1 summarizes 74.39 % of the information obtained with the two variables. The interpretation of the correlation circle between Henin's structural stability index and the plasticity index of the 20-40 cm horizon gives an angle equal to 60.66° less than 90° ($r_{Z_1 Z_2} = 0.49$), which means that these two variables are positively correlated.

  Only the relations between:

  - Henin's structural stability index and the liquidity limit of the horizon 0-20 cm,
  - Henin's structural stability index and the plasticity limit of the horizon 0-20 cm,
  - Henin's structural stability index and the plasticity index of the horizon 0-20 cm,

have a better correlation to the detriment of the 20-40 cm horizons.

Conclusion

The values of the Hénin structural stability index obtained in the horizon 0- 20 cm varies between 0.07 and 1.56 and for the horizon 20-40 cm the stability index of Henin varies between 0.23 to 2.22, this led us to conclude that the phenomenon of water erosion is not due to a lack of structural stability but rather results from intense runoff due to terrain. This explains why the horizons (0-20 cm) show the best correlations because this layer is more stressed and generates more fines than the horizon (20-40 cm).

References

[1]. Brown, L.R, Abramovitw, J., bright, C., Flaving, C., Gardner, G., Kane, H Platt, A., Postel, S., Roodman., D., sachs, A., et Starke L., L'etat de la planéte. Editions Economica, Paris-France, 1996.

[2]. Mamadou L. Lo, Alassane BA, Papa B.D. THIOUNE, Abdoulaye DIEDHIOU, EL Hadji B. DIAW, Water Erosion on the Thiés tray (Senegal): Study of the factors of the phenomenon using a Geotechnical Approach. Journal of scientific and Engineering Research, 5(4):220-230, 2018.

[3]. Cisse, S Tamba, ML. Lo, MB. Diop and G. Sissoko, 2012.Contribution to Improving the Performance of Concrete: The Case of use of Desert Sand of the region of Dakar. Research Journal of Environmental and Earth Sciences 4(12):1071-1078

[4]. Thierno O, Planchon O. (1999): La degradation des sols au sénégal: Analyse des methods d'inventaire et de l'utilisation des résultats. Bulletin Réseau Erosion, IRD, CTA, Montpellier, 155P.

[5]. Lo Mamadou Lamine, A. Ba, E.B. Diaw, A. Diéne, MB. Diop and G. Sissoko (2013).Technical studies of Treatment Basins and ravines of Area of Sanghe Senegal. Research journal of Environmental and Earth Sciences, 5(11), 660-670.

[6]. Carroll, J.D. (1968): Generalization of canonical analysis to three or more sets of variables, Proc. Am: Psych. Assoc., 227-228.

[7]. Besse, Ph. (1988): Spline functions and optimal metric in linear principal components analysis. In components and correspondence Analysis (Van Rijkevorsel et al, Eds.). Wiley, London.

[8]. Bernard, A, Guinot, C., Saporta, G. (2012) Sparse principal component analysis for multiblock data and its extension to sparse multiple correspondence analysis, Proceedings of Compstat 2012,99-106

[9]. Tremblay Denis et Vincent Robitaille (1994). Mécanique des sols Théorie et pratique 2^{iéme} édition, 472 p.

[10]. Hénin S., (1976). Cours de physique du sol. Orstom, Editest, 159p.

[11]. Musy André et Marc Soutter, (1991). Physique du sol Presses Polytechniques et Universitaires Romande (PPUR) collection: Gérer l'environnement: 348p.

[12]. Soutter, M., A. Mermoud et Musy A., Ingénierie des eaux et du sol Processus et aménagements, presse polytechniques et universitaires romandes, 316 p, 2007.